Cyclophanes

Deutsche Ausgabe: DOI: 10.1002/ange.201605997
Internationale Ausgabe: DOI: 10.1002/anie.201605997

Reversible Dimerization and Polymerization of a Janus Diradical To Produce Labile C–C Bonds and Large Chromic Effects

José L. Zafra, Lili Qiu, Naoyuki Yanai, Takamichi Mori, Masahiro Nakano, Miriam Peña Alvarez, Juan T. López Navarrete, Carlos J. Gómez-García, Miklos Kertesz, Kazuo Takimiya, and Juan Casado**

Abstract: *Conducting polymers can be synthesized by irreversible diradical monomer polymerization. A reversible version of this reaction consisting of the formation/dissociation of σ-dimers and σ-polymers from a stable quinonoidal diradical precursor is described. The reaction reversibility is made by a quinonoidal molecule which changes its structure to an aromatic species by forming weak and long intermolecular C–C single bonds. The reaction provokes a giant chromic effect of about 2.5 eV. The two opposite but complementary quinonoidal and aromatic tautomers provide the Janus faces of the reactants and products which produces the observed chromic effect. A reaction mechanism is proposed to explain the variety of final products starting with structurally very similar reactants. These reversible reactions, covering an unusual regime of weak covalent supramolecular bonding, yield products which might be envisaged as novel molecular and polymeric soft matter phases.*

Important conducting polymers,[1] such as poly(paraphenylene-vinylene),[2] are prepared by a diradical polymerization using monomers able to generate highly reactive quinonodimethane diradical intermediates,[3] which form strong chemically irreversible intermonomer C–C single bonds (Scheme 1). The reversible version of this polymerization mechanism is the subject of this work. Reversibly-made polymers might broaden the material versatility since one can move back and forth in the monomer/polymer equilibrium by mild external physical and environmental stimuli. The key aspect that differentiates the reversible and irreversible paths is the stability of the diradical intermediate. Therefore, a clear structure–property relationship is established: the more versatile molecular and polymeric reversibly-made materials should be based on highly stable diradical precursors.[4]

Chromism is a valuable property for functional materials,[5] and sometimes emerges as a manifestation of new underlying chemical phenomena. Some neutral monoradicals (imidazolyl[6] and phenalenyl[7] derivatives) and diradicals (diphenalenyls[8]) have been reported to show chromism by the formation of staircase π-stacking oligomers and polymers. Another related example is a tetrafluorobisimidazol quinonoidal compound which shows green to pale chromism promoted by a photochemical diradical dimerization (see Scheme S1 in the Supporting Information).[9] Nonetheless, the mediation of unpaired electrons is common in all these chromic reactions. Radical centers are capable of forming either multicenter delocalized pancake π-bonds or localized σ-bonds, the latter giving rise to unusually long fluxional C–C bonds.[10] In fact, σ- and π-products represent two competitive routes along the intermolecular dimerization/polymerization reaction pathway.[11,12] The result of the distinctive molecular reorganization after π- or σ-bonding provokes different chromic effects and is the subject of the present research.

Recently, tetracyanoquinonoidal oligothiophenes (Scheme 2) were intensively studied.[13,14] For those with a small number of thiophenes, the ground electronic state has a singlet closed-shell quinonoidal structure, whereas in the medium-sized members, the quinonoidal structure converts into a singlet open-shell diradical (Scheme 2).

We present here the reversible diradical σ-dimerization/σ-polymerization of the quinonoidal oligothiophene **1** (Schemes 1 and 2) triggered by mild stimuli (concentration, temperature, and pressure). The reaction is accompanied by a 2.5 eV chromic effect which originates from the transformation of its quinonoidal core in the monomer into an aromatic structure in the reaction products, a manifestation of the two-faced (Janus) nature of **1**. None of these changes have been detected for **2** (see Scheme 2).

The new quinonoidal compound **1** is prepared with two thiophenes fused to a naphthalene and bearing cyanoalkyloxycarbonyl-methylene functionalities at the outermost positions (see Scheme S2). In comparison with its dicyanomethylene counterpart **2**, the molecular optical properties, are

[*] Dr. J. L. Zafra, Prof. J. T. L. Navarrete, Prof. J. Casado
Department of Physical Chemistry, University of Málaga
29071 Málaga (Spain)
E-mail: casado@uma.es
L. Qiu, Prof. M. Kertesz
Department of Chemistry and Institute of Soft Matter
Georgetown University, Washington, D.C. 20057-1227 (USA)
N. Yanai, T. Mori
Department of Applied Chemistry, Graduate School of Engineering
Hiroshima University Kagamiyama
Higashi-Hiroshima 739-8527 (Japan)
T. Mori, Dr. M. Nakano, Prof. K. Takimiya
Emergent Molecular Function Research Group
RIKEN Center for Emergent Matter Science (CEMS)
2-1 Hirosawa, Wako, Saitama, 351-0198 (Japan)
E-mail: takimiya@riken.jp
Dr. M. P. Alvarez
Department of Physical Chemistry, Complutense University of Madrid, 28040 Madrid (Spain)
Prof. C. J. Gómez-García
Instituto de Ciencia Molecular, Universidad de Valencia
46980 Paterna, Valencia (Spain)

Supporting information for this article can be found under: http://dx.doi.org/10.1002/anie.201605997.

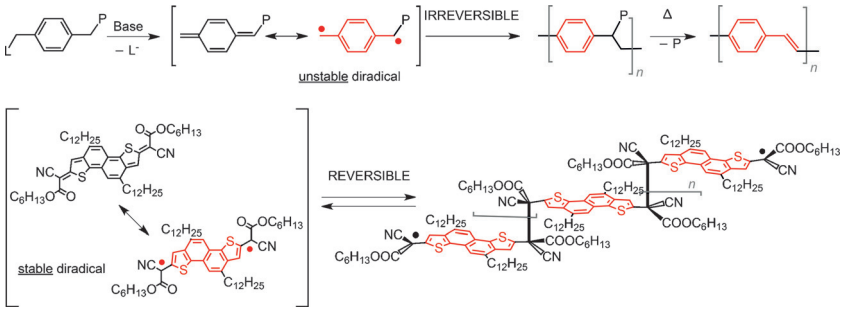

Scheme 1. Irreversible and reversible polymerizations in this study.

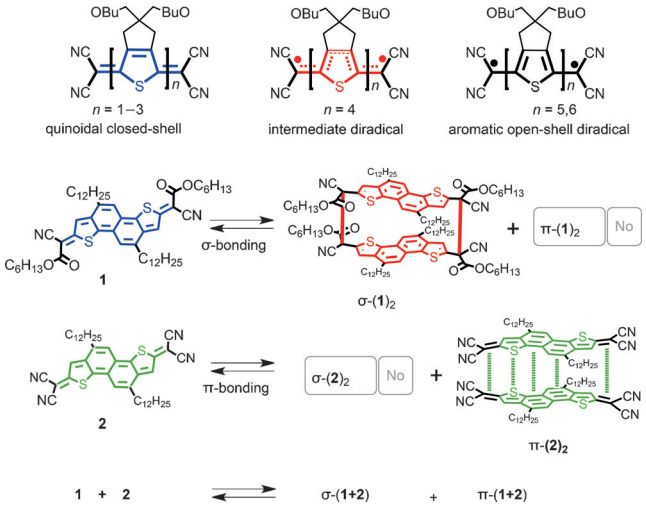

Scheme 2. From top to bottom: tetracyano quinonoidal oligothiophenes displaying sizeable diradical character and formation reactions of σ-($\mathbf{1}_2$), π-($\mathbf{2}_2$), σ-($\mathbf{1}+\mathbf{2}$), and π-($\mathbf{1}+\mathbf{2}$).

barely modified (Figure 1 a).[15,16] In fact, both **1** ($\lambda_{max}=$ 635 nm) and **2** ($\lambda_{max}=625$ nm) display very intense blue color in dichloromethane (CH_2Cl_2) solutions.

The unexpected result is that when **1** was deposited from solution by drop-casting as a thin solid film, it became completely colorless (see Movie S1), and fully recovers the blue color upon re-dissolution. Figure 1 b displays the UV/Vis absorption spectra of the thin film of **1** with main bands around $\lambda=270$–330 nm. The same chromic phenomenon is reproduced by starting with a dilute 10^{-5} M solution of **1** in CH_2Cl_2 and lowering the temperature (Figure 1 d; see Movie S2), thus observing again strong absorptions at $\lambda=$ 270–330 nm. In both cases, the emergence of these new bands was accompanied by the disappearance of the main absorption at $\lambda=635$ nm. When the frozen colorless solution was heated back to room temperature, the original blue band was fully re-established (Figure 1 d). The thermochromic cycle is reproduced in methylcyclohexane (C_7H_{14}) and in methyltetrahydrofurane (Me-THF). Heating the colorless thin film from room temperature allowed progressive recovery of the visible blue band at temperatures higher than 400 K (Figure 1 b). Finally, at room temperature similar UV/Vis spectral changes are observed when starting with a dilute solution of **1** and then increasing the concentration (Figure 1 c): at high concentrations, the bands at $\lambda=270$–330 nm increase to the detriment of the blue band. Compound **2** does not show any of these changes (see Figure S1).

Temperature-dependent experiments with dilute solutions allowed us, by assuming a dimerization process, to derive the thermodynamic parameters from the equilibrium constant $K(T)$ and by means of a van't Hoff plot [$K(T)$–$1/T$]. The variation of dimerization reaction enthalpy

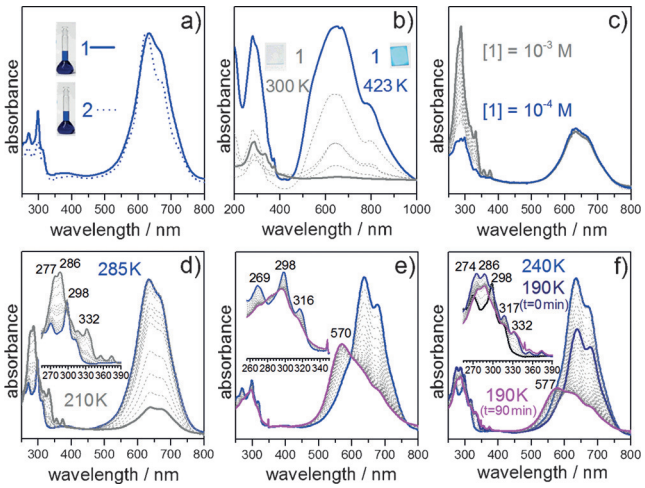

Figure 1. UV/Vis absorption characterization of the dimerizations: a) **1** and **2** at 300 K in 10^{-5} M solutions of CH_2Cl_2. b) **1** as a solid drop-cast thin film at 300 K (gray solid line) and after heating at 423 K for 90 minutes (blue solid line). c) Spectral evolution of a 10^{-4} M solution of **1** at room temperature (blue solid line) in CH_2Cl_2 with an increase on the concentration of up to 10^{-3} M (gray solid line). d) 10^{-5} M solution of **1** in CH_2Cl_2 by cooling. e) 10^{-5} M solution of **2** in CH_2Cl_2 by cooling from 285 K (blue line) to 190 K (pink line). f) 10^{-5} M equimolar solution of $\mathbf{1}+\mathbf{2}$ by cooling from 300 K to 190 K (after 90 minutes at 190 K).

($\Delta H°$) is obtained (Figure S2): −14.81 kcal mol^{-1} (CH_2Cl_2), −10.59 kcal mol^{-1} (C_7H_{14}), and −8.57 kcal mol^{-1} in (Me-THF). In addition, at 273 K the variation of the dimerization entropy, $\Delta S°$, is calculated: −0.048 kcal K^{-1} mol^{-1} in CH_2Cl_2, −0.065 kcal K^{-1} mol^{-1} in C_6H_{12}, and −0.058 kcal K^{-1} mol^{-1} in Me-THF. These data indicate that the exothermic character provides the driving force for the reaction.

The energetics of the dimerizations from quantum chemical calculations are summarized in Figure 2[17–19] (see Figures S3–S11 and Tables S1–S3). For the dimeric stacking configurations, we considered the *syn* and *anti* orientations with respect to the positions of the sulfur atoms, with the *anti* being more stable (except where indicated otherwise). We address two major *anti* isomers, σ- and π-dimers, for which several conformations have been modeled in Figure 2: 1) open or extended conformation [i.e., σ-($\mathbf{1}_2$)-op or π-($\mathbf{1}_2$)-op] with only one connection between the two monomers, 2) fully-closed conformation with face-to-face coupling [i.e.,

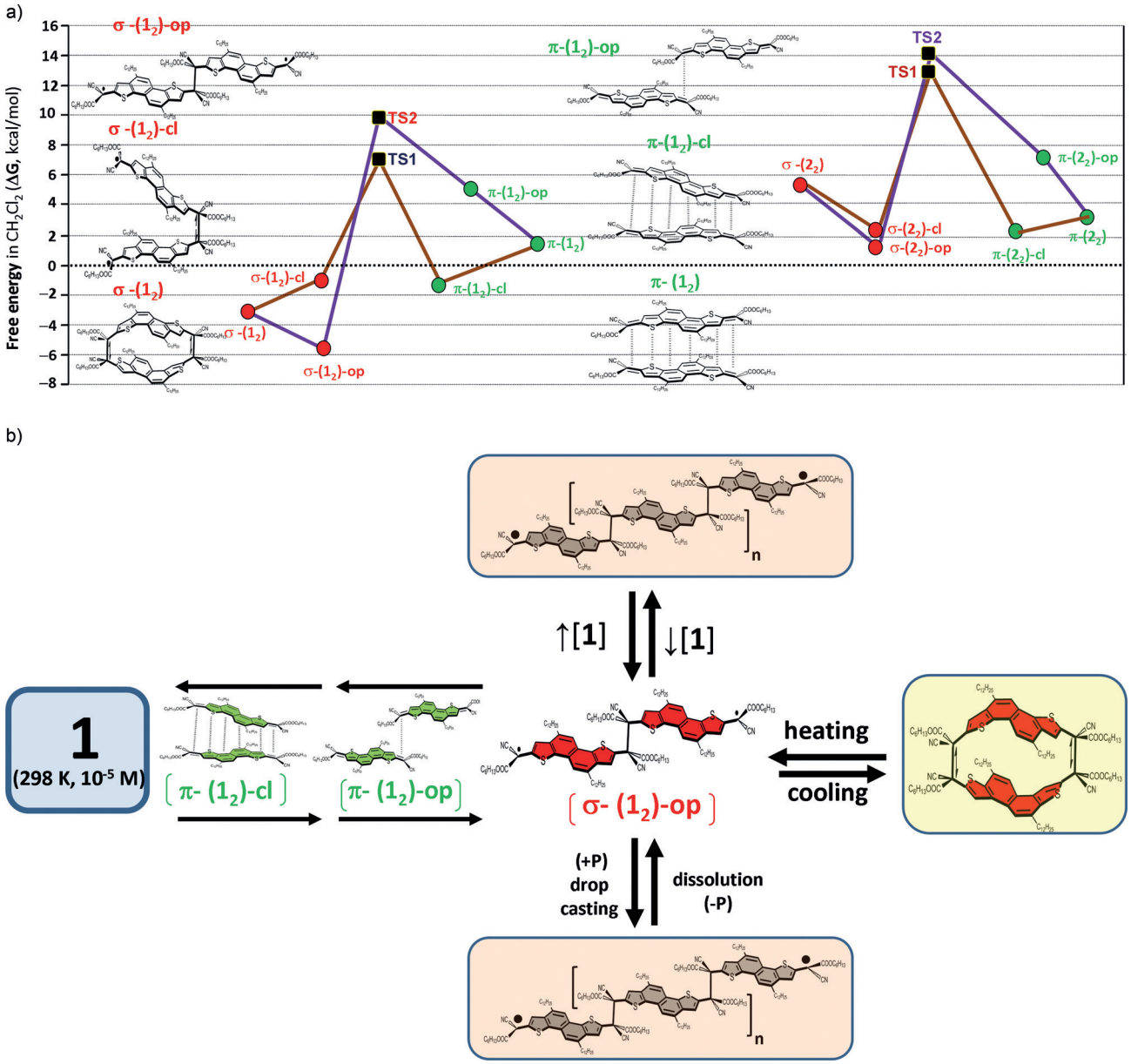

Figure 2. Calculated free-energy changes along the dimerization reaction (see the Supporting Information for details). Top: Relative Gibbs free energies ($\Delta G = G_{dimer} - 2\,G_{monomer}$) of each dimerization reaction of **1** (left) and **2** (right) in CH_2Cl_2. Lines are provided to guide the eye. All structures are local minima except the transition structures. Chemical structures represent the optimized geometries for **1** (structures for **2** are similar and not shown). TS (black squares) indicate the transition structures between the σ and π sides according to either the closed path (maroon line; TS1) or through an open route (purple line; TS2). Bottom: equilibria for σ-dimerizations and σ-polymerizations starting from π-dimerizations.

σ-(**1**$_2$) with two σ-bonding sites or π-(**1**$_2$) with pancake bonding], and 3) closed conformations [i.e., σ-(**1**$_2$)-cl or π-(**1**$_2$)-cl)] which are intermediate between the open and fully closed cases. Transition states have been also calculated between σ and π sides for **1** and **2**.

The relative Gibbs free energies (ΔG; Figure 2 and Table S3) have been calculated for each dimerization reaction and they are always negative for the formation of σ-dimers of **1**, thus revealing the spontaneous nature of the dimerization reactions. Among these reactions, the formation of σ-(**1**$_2$)-op is the most favorable. This favorability is in contrast to the endergonic character of the π-dimerizations of **1** (except for π-(**1**$_2$)-cl). For **2**, the formation of σ- and π-dimers is computed to be endergonic at 298 K, however, one would expect that a decrease of the temperature would promote their formation (exothermic reactions). The free-energy barriers towards the transition state for the σ↔π interconversion for **1** and **2** have been also evaluated and found that the smaller one is for the conversion from π-(**1**$_2$)-cl into σ-(**1**$_2$)-op, thus the solely stable π-dimer of **1** is certainly labile towards conversion into σ-bonded isomers. This reaction from π- to σ-dimers of **1** can go through two different mechanisms: an open or step-by-step route (maroon line in Figure 2) which first breaks the symmetry of the starting π-dimer [π-(**1**$_2$)] by forming

a singly π-bonded diradical [π-($\mathbf{1}_2$)-cl] and then via TS1 (Figure S10) is converted into the equivalent σ-($\mathbf{1}_2$)-cl; and a concerted path (purple line in Figure 2; see Figure S10), via TS2, which maintains the symmetry between the fragments during the reaction. Although the transition barrier via TS1 is smaller than via TS2 both mechanisms might be operative for the permanent fueling of σ-dimers. What is important is that dimers of **1** always form first and the labile π-dimers then evolve into σ-dimers through one or another path. For **2**, these barriers are larger and once π-dimers are formed they would be more persistent.

Calculations for monomers of **1** and **2** show significant diradical character (see Table S1), and it is enhanced and modulated by intermolecular interactions along the dimerization reaction coordinate, thus giving rise to dimer radicaloid species, such as σ-($\mathbf{1}_2$)-op, and from this closed-shell cyclophane dimers, such as σ-($\mathbf{1}_2$), are formed. For instance, **1** has a π-spin density of −0.4 e on the sp^2 carbon atoms adjacent to the CN groups (Tables S1 and S2) and they are cancelled in σ-($\mathbf{1}_2$) in the formation of long highly strained C–C single σ-bonds with computed lengths of 1.676 Å (see Figure S4).[20] In σ-($\mathbf{1}_2$)-op only one strained bond (1.623 Å; see Figure S6) is formed, thus leaving two unpaired electrons at the extremities. The structures of σ-($\mathbf{1}_2$) and σ-($\mathbf{1}_2$)-op feature aromatic substructures for the naphthalene and thiophene rings. For σ-($\mathbf{1}_2$), this central aromatic core is slightly bulging out (see Figure S4) to minimize steric repulsions. TD-DFT excited-state calculations for **1** and **2** and their dimers (see Figure S12) nicely reproduce the UV/Vis spectra in Figure 1, thus confirming that in **1** the dominant final product is σ-($\mathbf{1}_2$), while **2** is the trapped π-($\mathbf{2}_2$) species.

Temperature-dependent ^{1}H NMR data of **1** in a dilute solution are shown in Figure 3a. At room temperature two main peaks are assigned to the protons of the thiophene ($\delta =$ 7.19 ppm) and of the naphthalene ($\delta = 7.66$ ppm) featuring quinonoidal structures (monomer **1**). These signals progressively disappear upon cooling to give rise to multiple signals, which are mainly downfield, and are in-line with the formation of aromatic structures (see Figure S13). To characterize the open-shell structures, we have also carried out electron paramagnetic resonance (EPR) studies. The EPR spectrum of the dilute solution of **1** does not give any resolvable signal at any temperature (Figure 3b; see Figure S14). In contrast, the ^{1}H NMR spectrum of the 10^{-3} M concentrated solution of **1** at room temperature is shown in Figure 3c, and it is also characterized by two peaks, which are similarly placed downfield relative to the signals of the monomer **1** as a result of core aromatization. When this concentrated solution is analyzed by EPR spectroscopy, the room-temperature spectrum shows a well-resolved band with up to 15 lines (Figure 3d) resulting from the hyperfine coupling of the unpaired electrons with the thiophene and naphthalene H and N atoms (see Figure S15 and Table S4). The intensity of this signal progressively decreases as the temperature is lowered. This ^{1}H NMR/EPR behavior is consistent with the formation of an open-shell aromatic species such as σ-($\mathbf{1}_2$)-op in the concentrated solution. This species, upon cooling, can trap more monomers at the two termini, thus giving way to a propagation step towards the formation of long σ-oligomers or σ-polymers. In the dilute solution, σ-($\mathbf{1}_2$)-op might be also initially formed but it cannot react intermolecularly. However it reacts intramolecularly by reorienting the fragments to make a second strained single C–C bond in σ-($\mathbf{1}_2$), which is an EPR silent aromatic cyclophane species.

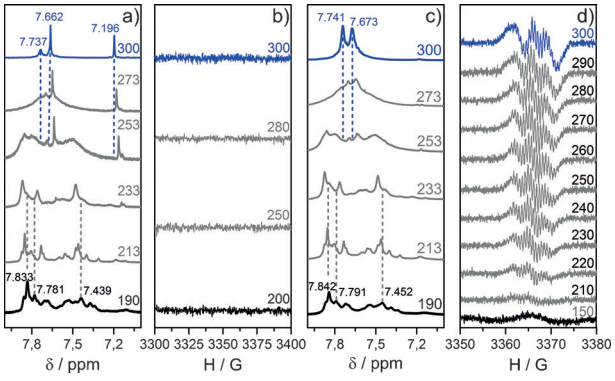

Figure 3. Variable-temperature ^{1}H NMR (a,c) in CD_2Cl_2 and EPR (b,d) in CH_2Cl_2 studies. a,b) For a 10^{-5} M solution of **1**. c,d) For a 10^{-3} M solution of **1**. Temperature is indicated in K.

The EPR study has also been carried out for the drop-cast thin solid film of **1**. At room temperature, it gives rise to a well-resolved doublet EPR signal[21] (see Figures S16 and S17) which increases in intensity by heating to 400 K, and it then progressively disappears when cooling to about 280 K in correspondence with the reversible formation (see Figure S18) of either a σ-oligomer or polymer at room temperature, and it is then destroyed by heating. This colorless thin solid film has also been analyzed by means of FTMS ICP mass spectrometry (see Figure S19) and found the strongest peaks resulting from oligomers of **1**.

An identical cooling process was carried out for a dilute solution of **2** and monitored by UV/Vis absorption (Figure 1e). At low temperatures, the main absorption band of the monomer develops a single new band at $\lambda = 570$ nm which gives a rosy-blush color to the cold solution. This $\lambda = 570$ nm band at low temperatures is predicted by TD-DFT calculations to be at $\lambda = 587$ nm for its π-dimer, π-($\mathbf{2}_2$) (see Figure S21) with no traces of σ-($\mathbf{2}_2$) in the spectra. In spite of the structural similarity, while **1** forms σ-($\mathbf{1}_2$), **2** forms π-($\mathbf{2}_2$), a behavior accounted for by the exoergic character of **1**↔σ-($\mathbf{1}_2$) [**2**↔σ-($\mathbf{2}_2$) is endergonic], whereas **2**↔π-($\mathbf{2}_2$) is quickly formed and kinetically trapped by large isomerization barriers. It seems that the occurrence in **1** of more soft vibrational modes might be at the origin of the different entropy contributions to the free energies resulting from the cyano→acyl replacement.

The formation of the σ-dimers of **1** and π-dimers of **2**, besides their chemical similarity, gives a good account of the delicate balance of forces intervening in these dimerizations. Therefore the question arises: would **1** + **2** form **1**-**2** σ-mixed dimers or alternatively **1**-**2** π-mixed dimers? Figure 1f shows the UV/Vis absorption spectra of an equimolar dilute mixture of **1** and **2** as the temperature is lowered (see Figure S21). We detect two regimes: 1) from 250 to 190 K where the intensities of the **1** and **2** monomer bands decrease, and two new bands

appear at $\lambda = 274$ nm and 287 nm. These values are close to those of σ-($\mathbf{1}_2$) but the slight difference likely reveals the formation of either a new species or the mixed σ-dimer σ-(**1** + **2**). 2) At 190 K, σ-(**1** + **2**) is seemingly unstable and its spectrum spontaneously evolves with time into a broad band at $\lambda = 577$ nm, which is within the range for bands of π-dimers, but again the slight difference from that assigned in π-($\mathbf{2}_2$), thus suggesting either a new π-dimer or π-(1 + 2). TD-DFT excited-state calculations in Figure S21 further corroborate the formation of these σ-(**1** + **2**) and π-(**1** + **2**) species.

Mechanochromism resulting from structural changes resulting from external pressure stimuli is a novel and valuable property of soft materials capable of forming aggregates. Raman spectroscopy is a very appropriate tool for pressure-dependent studies as it provides the molecular structural fingerprint under pressure. The Raman spectrum of the blue monomer of **1** in Figure 4 a.1 is typical of a quinonoid structure with a strong band around 1407 cm^{-1} resulting from

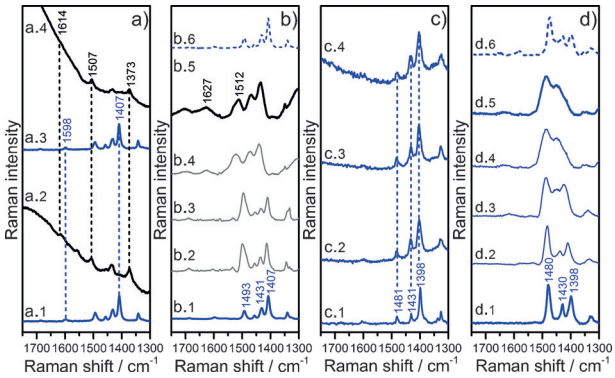

Figure 4. Solid-state Raman spectra of **1** and **2**. a) Powder of **1** (a.1), colorless drop-cast thin film from solution (a.2), the above thin film heated at 400 K (a.3), re-dissolved and re-deposited as a drop-cast film (a.4). b) Powder of **1** at different pressures (b.1), 1 GPa (b.2), 3 GPa (b.3), 5 GPa (b.4), 6 GPa (b.5), pressure release (b.6). c) The same as (a) for **2**. d) The same as (b) for **2**. Raman spectra in (a)/(c) are taken with the $\lambda = 532$ nm laser excitation and (b)/(d) with the $\lambda = 785$ nm one.

the quinonoidal thiophene C=C stretching modes, ν(C=C).[22] In the colorless drop-cast thin solid film resulting from the σ-polymer, the Raman spectrum completely changes and new bands at 1507/1614 cm^{-1} appear, and are typical of ν(C=C) from aromatic thiophenes and naphthalenes, respectively (see Figure S22). Variable-pressure Raman experiments have been conducted for **1** and **2** (Figure 4 b,d). **1** under about 6 GPa showed new Raman bands at 1510/20–1620 cm^{-1}, similar to those of the drop-cast σ-polymer, whereas in **2** no new bands are present in this pressure range. We address these Raman findings by assuming that under mechanical stress neighboring molecules of **1** are pushed closer, thus promoting the generation of the radicaloid σ-($\mathbf{1}_2$)-op intermediate which by σ reaction could produce an aromatic solid-state σ-polymer responsible for the high-pressure Raman spectrum. This behavior is not observed for **2** when exposed to pressure because of the instability of its σ-polymer.

In summary, we have reported the chemically reversible formation of σ-aggregates in solution and in the solid state for a stable quinonoidal molecule, a dimerization/polymerization reaction which provokes a shift of more than 2.5 eV of the electronic absorption bands and takes place upon exposure to thermal, concentration, and pressure stimuli. These quinonoidal naphthodithiophenes are able to form a variety of dimers: σ-($\mathbf{1}_2$) in the case of the cyanoester derivative, π-($\mathbf{2}_2$) for the dicyano case and, unexpectedly, both types for the mixed dimers, σ-(**1** + **2**) and π-(**1** + **2**). The two structural antagonistic faces of the quinonoidal(reactants) versus aromatic(products) transformation discloses an example of Janus-type molecules. The diradical σ-($\mathbf{1}_2$)-op dimer is the key intermediate which is formed first from unstable π-dimer intermediates and is able either to intramolecularly form a closed-shell σ-($\mathbf{1}_2$) cyclophane, or represent the first step of the propagation mechanism of the oligomerization/polymerization reaction. Thus, we have described a novel reaction to prepare reversibly-made chromic dimers and polymers, and propose a mechanism which aids in understanding the fundamental properties of the diverse aggregation modes of π-conjugated molecules. These soft materials can be envisaged for applications as novel molecular and polymeric soft matter phases.

Acknowledgments

We acknowledge support from MINECO/FEDER of Spanish Government (CTQ2012-33733 and CTQ2015-69391-P), Junta de Andalucía (P09-FQM-4708), and Generalitat Valenciana (Prometeo-II2014/076 and ISIC projects). J.L.Z. thanks the Research Central Services (SCAI) of the University of Málaga. This work was financially supported by JSPS KAKENHI Grant Number 15H02196 and by ImPACT Program of Council for Science, Technology and Innovation (Cabinet Office, Government of Japan). We thank the U.S. National Science Foundation (grant no. CHE-1006702, at Georgetown University). M.K. is member of the Georgetown Institute of Soft Matter.

Keywords: cyclophanes · density functional calculations · radicals · reaction mechanisms · solvatochromism

How to cite: *Angew. Chem. Int. Ed.* **2016**, *55*, 14563–14568
Angew. Chem. **2016**, *128*, 14783–14788

[1] J. Reynolds, *Handbook of Conducting Polymers*, 3rd ed. (Ed.: T. A. Skotheim), CRC Press, Boca Raton, FL, **2007**.
[2] A. Kraft, A. Grimsdale, A. Holmes, *Angew. Chem. Int. Ed.* **1998**, *37*, 402; *Angew. Chem.* **1998**, *110*, 416.
[3] N. J. Hoboken, *Principles of Polymerization*, 4th ed. (Ed.: G. Odian), Wiley, Hoboken, **2004**.
[4] G. Sonmez, F. Wudl, *J. Mater. Chem.* **2005**, *15*, 20.
[5] S. A. Jenekhe, D. J. Kiserow, *Chromogenic Phenomena in Polymers*, American Chemical Society, Washington, **2004**.
[6] S. Hatano, T. Horino, A. Tokita, T. Oshima, J. Abe, *J. Am. Chem. Soc.* **2013**, *135*, 3164.
[7] a) K. Goto, T. Kubo, K. Yamamoto, K. Nakasuji, K. Sato, D. Shiomi, T. Takui, M. Kubota, T. Kobayashi, K. Yakusi, J.

Ouyang, *J. Am. Chem. Soc.* **1999**, *121*, 1619; b) J. M. Lü, S. V. Rosokha, J. K. Kochi, *J. Am. Chem. Soc.* **2003**, *125*, 12161.
[8] a) T. Kubo, A. Shimizu, M. Sakamoto, M. Uruichi, K. Yakushi, M. Nakano, D. Shiomi, K. Sato, T. Yakui, Y. Morita, K. Nakasuji, *Angew. Chem. Int. Ed.* **2005**, *44*, 6564; *Angew. Chem.* **2005**, *117*, 6722; b) J. Huang, M. Kertesz, *J. Am. Chem. Soc.* **2007**, *129*, 1634.
[9] A. Kikuchi, F. Iwahori, J. Abe, *J. Am. Chem. Soc.* **2004**, *126*, 6526.
[10] A. Shimizu, M. Uruichi, K. Yakushi, H. Matsuzaki, H. Okamoto, M. Nakano, Y. Hirao, K. Matsumoto, H. Kurata, T. Kubo, *Angew. Chem. Int. Ed.* **2009**, *48*, 5482; *Angew. Chem.* **2009**, *121*, 5590.
[11] Z.-H. Cui, H. Lischka, H. Z. Beneberu, M. Kertesz, *J. Am. Chem. Soc.* **2014**, *136*, 12958.
[12] Z. Mou, K. Uchida, T. Kubo, M. Kertesz, *J. Am. Chem. Soc.* **2014**, *136*, 18009.
[13] R. Ponce Ortiz, J. Casado, V. Hernández, J. T. López Navarrete, P. M. Viruela, E. Ortí, K. Takimiya, T. Otsubo, *Angew. Chem. Int. Ed.* **2007**, *46*, 9057; *Angew. Chem.* **2007**, *119*, 9215.
[14] J. Casado, R. Ponce Ortiz, J. T. López Navarrete, *Chem. Soc. Rev.* **2012**, *41*, 5672.
[15] T. Mori, N. Yanai, I. Osaka, K. Takimiya, *Org. Lett.* **2014**, *16*, 1334.
[16] Y. Suzuki, E. Miyazaki, K. Takimiya, *J. Am. Chem. Soc.* **2010**, *132*, 10453.
[17] R. G. Parr, W. Yang, *Density-Functional Theory of Atoms and Molecules*, Oxford University Press, Oxford, **1989**.
[18] Y. Zhao, D. G. Truhlar, *Theor. Chem. Acc.* **2008**, *120*, 215.
[19] G. A. Petersson, A. Bennett, T. G. Tensfeldt, M. A. Al-Laham, W. A. Shirley, J. Mantzaris, *J. Chem. Phys.* **1988**, *89*, 2193.
[20] A few extremely stretched long C–C bonds above 1.7 Å have been reported. See, for example: F. Toda, K. Tanaka, Z. Stein, I. Goldberg, *Acta Crystallogr. Sect. C* **1996**, *52*, 177.
[21] The EPR analysis provides more evidence if a solution more concentrated than 3 mg mL^{-1} is studied. Its EPR signal consists of a doublet assigned to the hyperfine couplings of the diradical only with the thiophene and naphthalene H atoms (not with the N atoms). We can attribute this coupling to the concurrent $sp^2 \rightarrow sp^3$ pyramidalization of the carbon atoms as they form the long C–C bonds which decouple the π-electron density of the external cyano groups from the central core.
[22] V. Hernández, S. Hotta, J. T. López Navarrete, *J. Chem. Phys.* **1998**, *109*, 2543.

Received: June 20, 2016
Published online: October 26, 2016

